Intracellular Locations of Replication Proteins and the Origin of Replication during Chromosome Duplication in the Slowly Growing Human Pathogen *Helicobacter pylori*

Atul Sharma,[a] Mohammad Kamran,[a] Vijay Verma,[a] Santanu Dasgupta,[b] Suman Kumar Dhar[a]

Special Centre for Molecular Medicine, Jawaharlal Nehru University, New Delhi, India[a]; Department of Cell and Molecular Biology, Uppsala University, Uppsala, Sweden[b]

We followed the position of the replication complex in the pathogenic bacterium *Helicobacter pylori* using antibodies raised against the single-stranded DNA binding protein (HpSSB) and the replicative helicase (HpDnaB). The position of the replication origin, *oriC*, was also localized in growing cells by fluorescence *in situ* hybridization (FISH) with fluorescence-labeled DNA sequences adjacent to the origin. The replisome assembled at *oriC* near one of the cell poles, and the two forks moved together toward the cell center as replication progressed in the growing cell. Termination and resolution of the forks occurred near midcell, on one side of the septal membrane. The duplicated copies of *oriC* did not separate until late in elongation, when the daughter chromosomes segregated into bilobed nucleoids, suggesting sister chromatid cohesion at or near the *oriC* region. Components of the replication machinery, *viz.*, HpDnaB and HpDnaG (DNA primase), were found associated with the cell membrane. A model for the assembly and location of the *H. pylori* replication machinery during chromosomal duplication is presented.

Helicobacter pylori is possibly the most common human pathogen, affecting almost half of the world's population. *H. pylori* infection can cause chronic gastritis leading to gastric ulcers, intestinal metaplasia, and adenocarcinoma (1–3). Its spiral shape and unipolar flagella give the pathogen the motility critically needed to colonize and persist in the gastric lumen. *H. pylori* has developed unique sets of genetic and physiological tools to survive and grow in the extremes of the human gastric environment (4–8). Moreover, it can transform itself from a helical bacillary morphology to a viable but nonculturable coccoid form under oxidative stress and in ageing cultures (9). The signals eliciting the bimorphic response and the molecular mechanisms bringing about the transformation are not known. An intimate knowledge of cell cycle controls, including those of chromosome replication and cell division, is necessary for an understanding of these processes. However, very little is known about chromosome replication and its coordination with growth and division in *H. pylori*.

Several components of the *H. pylori* replication machinery have already been characterized, *viz.*, the initiator DnaA, the replicative helicase DnaB, the single-stranded DNA binding protein SSB and the primase DnaG (10–13). The *H. pylori* replication origin, Hp*oriC*, has also been identified in the *H. pylori* chromosome. The initiator protein HpDnaA binds to the unique bipartite replication origin Hp*oriC* and initiates DNA unwinding *in vitro* (14). Recently, a unique DnaA binding protein, HobA, has been identified as the regulator of the timing and frequency of DnaA-dependent initiation from *oriC* by aiding the oligomerization of DnaA for orisome (a multiprotein complex formed at the *oriC*) assembly at Hp*oriC*, analogous to DiaA function in *Escherichia coli* (15).

There are features of replisome assembly that distinguish *H. pylori* from the conventional model systems, such as *E. coli* or *Bacillus subtilis*. The HpDnaB helicase has been shown to complement the helicase loader function of DnaC in *E. coli in vivo* (16), suggesting a self-loading function of HpDnaB consistent with the

absence of a *dnaC*-like gene in the *H. pylori* genome. The C-terminal region of HpDnaB contains an insertion of ~34 amino acids, relative to *E. coli* DnaB, that is essential for its function (17). The single-stranded DNA binding protein (HpSSB) plays a central role in DNA replication by modulating DnaB helicase activity. HpSSB and HpDnaB form replication foci that may help differentiate the replicationally active helical form and the dormant coccoid form of *H. pylori* (12).

Though the replication proteins forming the replisome are functionally conserved, their intracellular organization varies among bacteria depending on their living environments, cell physiologies, and growth rates (18–21). The important aspects of replisome dynamics and cell cycle control in *H. pylori* remain elusive. As a slowly growing pathogen surviving in a special ecological niche, *H. pylori* may show some unique features in the assembly of its replisome and its functional dynamics during the cell cycle. We followed the locations of the replisome, using HpSSB foci as reporters for replication sites in fixed *H. pylori* cells at different stages of growth and division. We show that in *H. pylori* cells from a growing culture, the majority of replication foci localize at the cell poles, not around the midcell, as seen in *E. coli* (22–24) and in *B. subtilis* (25). Colocalization of the HpDnaB helicase with the HpSSB validated the identity of the SSB foci as active replication centers that moved from pole proximal to the midcell region with increasing cell size. The replication origin,

TABLE 1 Bacterial strains and plasmids

Bacterial strain/plasmid	Genotype/relevant characteristics	Source
E. coli strains		
DH10β	F⁻ *mcrA* Δ(*mrr-hsdRMS mcrBC*) φ80d*lacZ*ΔM15 Δ*lacX74 recA1 endA1 araD139* Δ(*ara leu*)7697 *galU galK* λ⁻ *rpsL nupG*	Molecular Cloning Laboratories (MCLAB)
BL21(DE3)	F⁻ *ompT hsdS*$_B$(r$_B^-$ m$_B^-$) *gal dcm* (DE3)	Novagen
H. pylori strains		
26695	ATCC 700392	ATCC
B28	Strain isolated from Indian patient at NICED, Kolkata, India	A. Mukhopadhyay
Plasmids		
pET28a	T7 *his kanR*	Novagen
pET28aHpFlgE	pET28a derivative containing 700 bp of *H. pylori flgE*	This study

oriC, was localized by fluorescence *in situ* hybridization (FISH) with *oriC*-proximal DNA sequences as probes. Subcellular fractionation revealed DnaB helicase and DnaG primase to be associated with the *H. pylori* cell membrane fraction, whereas most of the HpSSB was found in the soluble cytoplasmic fraction. Immunogold electron microscopy (EM) confirmed membrane association and polar localization of some replication proteins. The polar location of the replication complex, association of the active replisome with the bacterial cell membrane, and the presence of a probable centromeric region near the bipartite *oriC* appear to be some of the hitherto unknown features of *H. pylori* chromosome replication.

MATERIALS AND METHODS

Bacterial strains and plasmids. The bacterial strains and plasmids used in this study are listed in Table 1.

Growth conditions of bacterial cultures. *E. coli* strains were grown in Luria broth (LB) medium (supplemented with 100 μg/ml ampicillin or 50 μg/ml kanamycin where needed) at 37°C or 22°C. The *E. coli* cells were grown on LB agar plates (with or without antibiotics, as appropriate) at 37°C for 12 to 16 h.

H. pylori strain 26695 was grown on brain heart infusion (BHI) agar (Difco, Sparks, MD, USA) supplemented with 7% horse blood serum (Gibco, Invitrogen), 0.4% IsoVitaleX (Becton Dickinson, USA). The antibiotics used, when needed, were amphotericin B (8 μg/ml), trimethoprim (5 μg/ml), and vancomycin (10 μg/ml). The plates were incubated at 37°C under microaerobic conditions (5% O$_2$, 10% CO$_2$) using the Gaspak100 system (Becton Dickinson, USA) for 24 to 48 h, as required. BHI broth (Difco, USA) with 10% horse blood serum, 0.4% IsoVitaleX and antibiotics, as described above, was used for liquid culture. The cells from the liquid culture were harvested for experiments after 36 to 48 h. All antibiotics were from Sigma Chemicals USA.

DNA manipulations and cloning of the gene coding for HpFlgE. The coding sequence of the open reading frame (ORF) HP0870 (annotated as the putative gene encoding HpFlgE, the flagellar protein of *H. pylori*) was amplified by using specific forward and reverse primers (Fw, 5′ CCCCA TATGAACGACACCTTATTAAACGC 3′, and Rv, 5′ CGGGATCCTTAT TTTTTCAAGCTAATGGCTTC 3′) and the genomic DNA from *H. pylori* strain 26695 as the template. The amplified PCR product was cloned into the NdeI-BamHI restriction sites of the expression vector pET28a in *E. coli* strain DH10β (Table 1). The recombinant clone was verified by PCR and by sequencing.

Protein expression and purification and antibody generation. *E. coli* strain BL21(DE3) (Novagen) harboring pET28a HpFlgE (wild type [WT]) was grown at 37°C in LB medium containing kanamycin. Expression of the recombinant protein was induced at an optical density at 600 nm (OD$_{600}$) of ∼0.4 by adding 0.25 mM IPTG (isopropyl-β-D-thiogalactopyranoside) and allowing the culture to grow at 22°C. The His$_6$-tagged protein was purified using Ni-nitrilotriacetic acid (NTA) agarose beads (Qiagen, Hilden, Germany) according to the manufacturer's instructions. The eluted protein was dialyzed against the buffer containing 50 mM Tris-HCl (pH 7.5), 1 mM EDTA, 100 mM NaCl, 100 mM phenylmethanesulfonyl fluoride (PMSF), and 10% glycerol. The dialyzed protein was checked for purity by SDS-PAGE analysis. Protein concentrations were determined by the Bradford method (Bio-Rad, Hercules, CA, USA), in accordance with the manufacturer's instructions, with bovine serum albumin (BSA) as a standard. Polyclonal antibodies were raised in rabbits against His$_6$-HpFlgE using the protocol of Harlow and Lane (26). The specificity of the antiserum was checked by Western blotting using *H. pylori* extract and recombinant protein. We previously described the generation of polyclonal antibodies raised against HpDnaB and HpSSB (11, 12), the cloning of the coding region of HpDnaG (ORF 0012), and the purification of the His$_6$-HpDnaG protein (13). Polyclonal antibodies in mice were raised against His$_6$-HpDnaG according to a protocol described previously (26).

Western blotting. Western blotting was used to measure the expression of HpFlgE in the bacterial lysate, as well as to check the specificity of the antibodies generated against the recombinant proteins. Recombinant proteins (100 ng each) or bacterial cell lysate (∼100 to 200 μg) was boiled in 1× SDS gel loading buffer at 95°C for 5 min, resolved by electrophoresis in a 10% polyacrylamide-SDS gel, and transferred to polyvinylidene difluoride (PVDF) membranes (Amersham Biosciences, Uppsala, Sweden). The blots were blocked with 5% nonfat skim milk powder for 1 h at room temperature in phosphate-buffered saline–Tween 20 (PBST), followed by three 5-min washes with PBST. After washing, the blots were probed with anti-HpFlgE (rabbit) antibodies for 1 h at room temperature, followed by three washes of 10 min each with PBST. Horseradish peroxidase (HRP)-conjugated anti-rabbit secondary antibodies were added to the corresponding blots and incubated further for 45 to 60 min at room temperature. The blots were washed three times with PBST to remove the nonspecifically bound secondary antibodies. Finally, the blots were developed by using the ECL + Western blotting detection system (Amersham Biosciences, Uppsala, Sweden).

For Western blot analysis of *H. pylori* cell fractions, *H. pylori* cell lysate, cytosolic fractions, or membrane fractions were mixed with an equal volume of 2× SDS loading dye and boiled at 95°C for 5 min. The samples were subjected to 12% SDS-PAGE, transferred to a PVDF membrane (Amersham Biosciences), and subsequently processed for Western blotting as described above using specific antibodies against HpSSB (mice), HpDnaG (mice), or HpDnaB (rabbit).

Immunofluorescence microscopy. *H. pylori* cells were harvested from plates or liquid culture and washed three times with 1× PBS to remove traces of the growth medium. The cells were then fixed with 4% paraformaldehyde in 1× PBS for 15 min at room temperature. The fixed cell suspension was spread on poly-L-lysine-coated glass slides and allowed to air dry. The cells were then washed with 1× PBS and treated with permeabilization buffer (20 mM Tris-HCl, pH 8.0, and 0.3% Triton X-100) for 20 min at room temperature; further washed with 1× PBS; and blocked with blocking buffer (2% BSA in 1× PBS). The cells were then incubated in blocking buffer at 4°C overnight with primary antibodies against HpSSB (mice), HpDnaB (rabbit), or HpFlgE (rabbit) separately or in combination, as required (1:500 dilution). The next day, after washing with 1× PBS, the cells were incubated with conjugated secondary antibodies, such as anti-mouse Alexa Fluor 594 (1:1,000) or anti-rabbit Alexa Fluor 488 (1:1,000), along with 4′,6-diamidino-2-phenylindole (DAPI) at a final concentration of 2 μg ml⁻¹. In order to examine colocalization,

cells were treated with two antibodies together. The membrane-staining dye FM 1-43FX was used at a final concentration of 1.5 μg ml^{-1} wherever required. All the fluorescence-tagged secondary antibodies, DAPI, and FM 1-43FX dye were from Molecular Probes-Invitrogen. Imaging was performed using a fluorescence microscope (Axioimager.Z1; Carl Zeiss Micro Imaging, Germany) equipped with an Axiocam HRm charge-coupled-device (CCD) camera under an ×100 magnification objective. Axiovision software (AxioVision LE v4.8; Carl Zeiss) and Adobe Photoshop 7.0 software were used for image analysis and image processing.

Generation time calculation. *H. pylori* cells were inoculated into the liquid BHI broth from an ~36-h plate culture and incubated at 37°C with continuous shaking (125 rpm). Aliquots were taken out at regular time intervals, and ODs were measured at 600 nm. To calculate the generation time, the log$_2$ OD was plotted against time, and the slope was calculated from the linear range (see Fig. S3 in the supplemental material). This slope is the growth rate of the culture (log$_2$ A_{600} h^{-1}); the inverse of the slope is the generation time (t_g).

EdU labeling. Twenty micromolar EdU (5-ethynyl-2′-deoxyuridine) (Molecular Probes) was added to growing *H. pylori* cultures, followed by incubation at 37°C for ~8 to 10 h. After washing with 1× PBS three times, the cells were fixed with 3.7% formaldehyde and air dried on poly-L-lysine-coated glass slides. Detection of EdU-labeled cells in the sample was performed by using an EDU Click-iT EdU Imaging Kit with Alexa 488-Green fluor (Molecular Probes-Invitrogen catalog no. C10337). DAPI at a concentration of 2 μg/ml was used in mounting medium to stain the nucleoids of the bacterial cells.

Fluorescence microscopy was performed as described in "Immunofluorescence microscopy" above. Two types of negative controls were used to ensure that the detected fluorescence was due to real signals from incorporated EdU: either cells were not incubated with EdU, or EdU-labeled cells were not treated with reaction buffer. Neither negative control showed any fluorescence signals, whereas the test slides showed punctuated fluorescent dots specifically attached to DAPI-stained nucleoid.

FISH. A 500-bp DNA fragment containing a putative Hp*oriC* region was PCR amplified from *H. pylori* 26695 genomic DNA using forward and reverse primers (Hp*oriC*Fw, 5′ GGCGTTATTATAGCGTG AATA 3′, and Hp*oriC*Rv, 5′CATTTTTTTAGCGAACATTTC3′, respectively). These primers were designed to amplify the 500-bp region of the chromosome upstream of the DnaA box sequences containing the putative Hp*oriC* (14). The purified PCR product was prepared as a probe using a fluorescence *in situ* hybridization multicolor kit with Alexa Fluor 594 dye or Alexa Fluor 488 dye (Invitrogen Inc., USA), following the manufacturer's instructions. For hybridization of the fluorescence-labeled probe with bacterial chromosomal DNA, a previously described protocol was followed (27). Briefly, 10 μl of the fixed cell suspension was spread on a poly-L-lysine-coated glass slide and air dried at room temperature. The sample slide was incubated in denaturing solution (70% formamide, 2× SSC [1× SSC is 0.15 M NaCl plus 0.015 M sodium citrate] at 75°C for 2 min, transferred to prechilled 70% ethanol, and kept for 5 min. The slide was then passed through a series of ethanol baths (90% and then 100%) for 5 min each and dried. The slide was covered with freshly prepared lysozyme solution (25 mM Tris-HCl, pH 8.0, 10 mM EDTA, 50 mM glucose, 2 mg/ml lysozyme) and incubated at room temperature for 10 min. The slide was washed in PBS (pH 7.5) for 5 min and transferred into a series of ethanol baths (70% and then 100% for 5 min each) and dried. The slide was then incubated overnight at 42°C with hybridization buffer (supplied by the vendor) containing the denatured probe. After hybridization, the slide was first washed in wash buffer (50% formamide, 2× SSC) at 37°C for 10 min and then with a series of SSC solutions (2×, 1×, 0.5×, and 1×) at room temperature for 5 min each. The slide was then washed in PBS containing 10 mM EDTA for 5 min and finally rinsed thoroughly with distilled water. The slide was air dried and fixed with a glass coverslip using mounting medium containing DAPI (supplied by the vendor). The slides were later observed using a Zeiss fluorescence microscope as described above.

Immunoelectron microscopy. Immunogold labeling was performed following a protocol described previously (28). *H. pylori* cells from growing cultures were harvested and fixed with 0.2% gluteraldehyde and 4% paraformaldehyde in 1× phosphate buffer (PB) (pH 7.5) for 1 h at 4°C and centrifuged at 10,000 × *g*, and the cell pellet was further fixed with 4% paraformaldehyde. After centrifugation at 10,000 × *g*, the cell pellet was washed two times with 1× PB (pH 7.5). The samples were dehydrated in ascending grades of ethanol and then infiltrated and embedded in LR White resin (TAAB, United Kingdom). Thin sections (1 μm) were then cut with an ultramicrotome and mounted on 300 mesh nickel grids. The grids were first incubated in cold 1% fish gelatin for 30 min to block nonspecific reactions. After this, the grids were further incubated overnight with primary antibodies against SSB, DnaB, and DnaG at 4°C using 0.01 M PBS and 1% fish gelatin as diluents at a 1:500 ratio. The next day, the grids were washed with diluents and then incubated with the respective secondary antibody conjugated with 10 nm colloidal gold for 2 h at room temperature. After labeling, the grids were washed thoroughly with 1× PBS and distilled water to remove the unbound antibodies and granules. The grids were then stained with uranyl acetate for 5 min, rinsed with distilled water, and blotted dry with filter paper. A JEOL 2100-F transmission electron microscope (JEOL, Japan) was used to observe the grids at magnifications of ×12,000 to ×25,000, and images of the cells with deposition of the gold particles were recorded. The preimmune sera against the above-mentioned proteins were used as negative controls.

Subcellular fractionation. *H. pylori* cell fractionation was carried out according to methods described previously (29–32). Briefly, *H. pylori* cells were harvested from growing plates or liquid culture (24 to 48 h). The 1.5-g cell pellet was washed and resuspended in 20 mM Tris-HCl (pH 8.0) and kept at 4°C for 30 min. Bacterial cells were lysed by ultrasonication (4 30-s pulses) and centrifuged at 7,000 × *g* for 10 min to remove unlysed cells and cell debris. The supernatant was collected, protease inhibitor cocktail was added, and the mixture was incubated at room temperature for 30 min. The lysate was subjected to ultracentrifugation (45 min; 130,000 × *g*) at 4°C. The supernatant containing the soluble cytoplasmic fractions was collected carefully without disturbing the pellet. The pellet containing the membrane fraction was washed two times in 1× PBS (pH 7.5) and resuspended in an equal volume of 20 mM Tris-HCl (pH 8.0). Both fractions were collected and stored as 20-μl samples. The total cell lysate, cytosolic fractions, and membrane fractions were each mixed with 2× SDS-PAGE loading buffer and electrophoresed on SDS-PAGE gels, followed by Western blotting using HpSSB, HpDnaB, and HpDnaG antibodies. We used the antibody against *H. pylori* heat shock protein (HSP) (sc-57779; Santa Cruz Biotech, Inc.) as a quantitative control for the total cytosolic protein loaded on the gel.

RESULTS

SSB foci represent replication sites in *H. pylori*. Active replication forks generally have extensive stretches of single-stranded DNA on the lagging-strand template, as well as somewhat shorter single-stranded regions on the leading-strand template behind the replicative helicase (33). The single-strand binding protein SSB can therefore be an excellent reporter for the ongoing replication sites in cells. This has been demonstrated convincingly in recent studies on localization of replication machines/factories or replisomes in *E. coli* (23, 24, 34). In order to record the location of the replication complex in *H. pylori*, we visualized fixed *H. pylori* cells taken from exponentially growing cultures by immunofluorescence microscopy using specific antibodies raised against HpSSB. Only ~6% of the cells showed distinct SSB foci, but no defined foci could be detected in cells that had reached the dormant coccoid forms (12). DAPI staining showed the positions of the SSB foci relative to the bacterial nucleoid or the folded bacterial chromosome(s).

A majority of the cells exhibiting SSB foci (~6% of the total number of cells counted) with one nucleoid had one replication focus located near
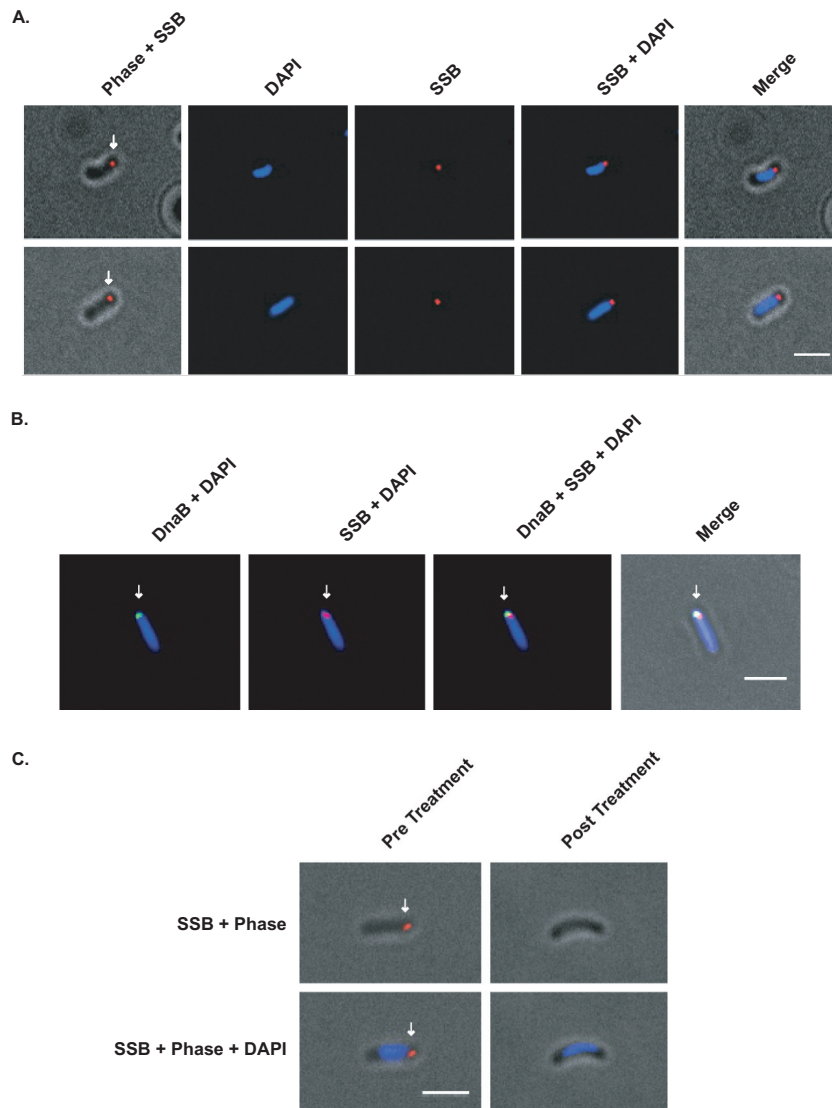
A.

B.

C.

FIG 1 Polar localization of the replisome in *H. pylori* cells. (A) Immunofluorescence images of fixed *H. pylori* cells treated with anti-HpSSB antibody show the localization of single SSB foci near the cell pole. DAPI fluorescence shows the nucleoid; the images at the extreme right show merged DAPI and SSB fluorescence superimposed on phase-contrast. The arrows mark the positions of the replication foci. (B) Colocalization of immunofluorescence from antibodies against HpDnaB and HpSSB at the cell pole indicates the positions of the replication foci. The image on the far right shows merged DAPI, SSB, and DnaB fluorescence superimposed on phase-contrast. (C) Loss of SSB fluorescence following treatment of *H. pylori* cells with the replication inhibitor novobiocin. Cells obtained from growing liquid culture before and after treatment with novobiocin were used for the immunofluorescence assay using antibodies against SSB. Scale bars, 2 μm.

one pole (Fig. 1A and Table 2). Immunolocalization experiments using polyclonal antibodies against both HpSSB and HpDnaB in the same cell showed that they were colocalized (Fig. 1B), suggesting that SSB foci are indeed present at replication complexes. Similar immuno-

TABLE 2 Frequencies of SSB foci based on immunofluorescence assays[a]

Pattern	No. of cells	%
Single polar focus	239	48.77
Single middle focus	163	33.26
Double foci	46	9.38
Multiple foci	42	8.57
Total no. of cells	490	100

[a] A total of 7,950 cells were scanned, 490 (~6.1%) of which showed SSB foci.

fluorescence assays (IFA) using preimmune sera did not show any foci (data not shown). Furthermore, a 30-min treatment of *H. pylori* culture with the gyrase-inhibiting drug novobiocin (35, 36) resulted in less than 0.5% of the cells bearing SSB foci (Fig. 1C). Novobiocin stops DNA replication and cell division rapidly. As the effect of the drug is reversible, washing out the antibiotic allowed the cells to restart replication, and SSB foci reappeared in these cells at the original pretreatment frequency of ~6% (data not shown). Together, these data indicate that the SSB foci are located at the active replication sites of ongoing DNA synthesis.

Intracellular locations of the replication sites. The number and intracellular distributions of the replication foci in *H. pylori* cells from cultures in exponential phase could be categorized into
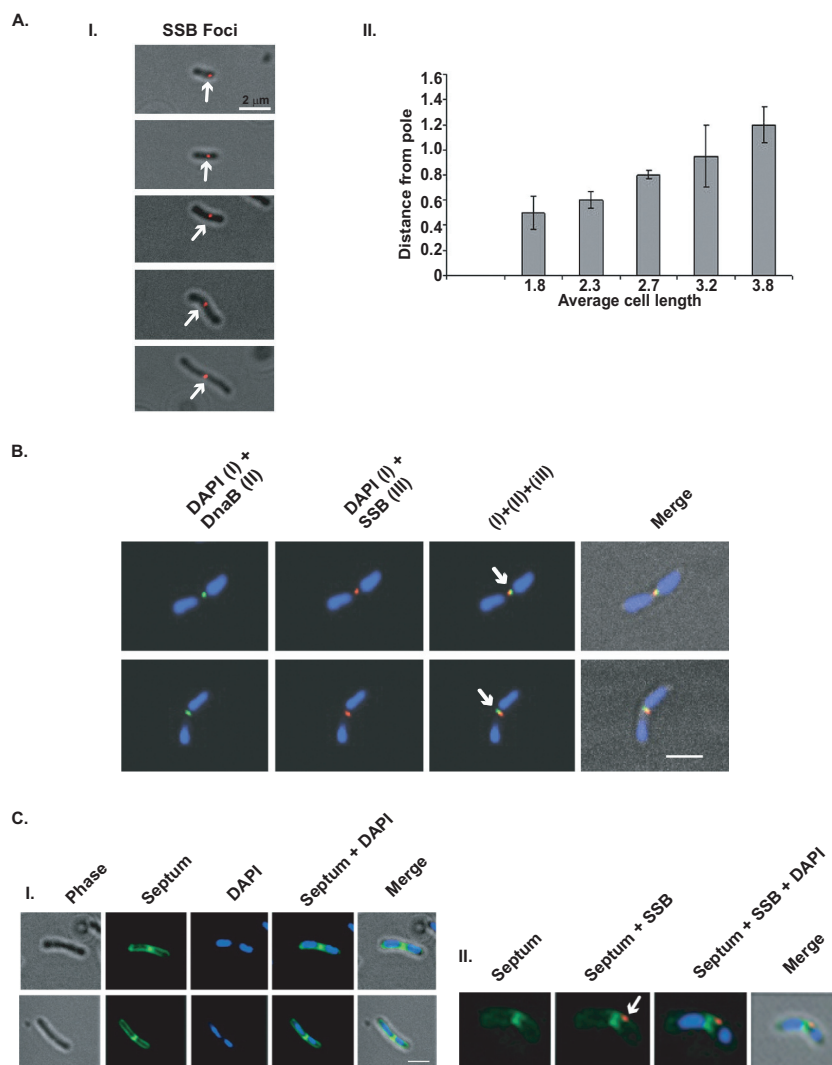
FIG 2 Changing positions of SSB foci as a function of cell length. (A-I) Localization of SSB foci with respect to cell length; the cells are placed in order of increasing size from top to bottom, with the SSB foci marked with arrows. (A-II) Average distances of SSB foci from one end in different cell length categories as a function of cell length. The error bars indicate standard errors. (B) Colocalization of HpSSB and HpDnaB fluorescence in binucleoid *H. pylori* cells stained with DAPI. The images on the extreme right show the merged fluorescence superimposed on the phase-contrast image. (C) Positions of cell septa in dividing *H. pylori* cells. (I) Fixed *H. pylori* cells were stained with the membrane marker dye FM 1-43FX and the DNA marker dye DAPI to visualize the relative positions of cell septa and nucleoids in dividing cells. (II) Asymmetric positions of HpSSB foci relative to a cell septum stained by FM 1-43FX dye in *H. pylori* cells containing two nucleoids; the replication foci (arrow) appear more closely attached to one nucleoid than the other. The image on the far right shows merged FM 1-43FX, DAPI, and SSB fluorescence superimposed on phase-contrast. Scale bars, 2 μm.

several groups, as shown in Fig. 2 and quantified in Table 2. Of all the cells with an SSB focus (490 out of 7,950 examined), about 82% had a single focus and about 18% had more than one focus. About 49% of the cells had the single replication focus located between the pole-proximal edge and the middle of the single nucleoid near the midcell position; about 33% had the focus near the midcell between two nucleoids with or without a visible cell division constriction site. Relatively few cells showed double (~9.4%) and multiple (~8.6%) foci (Table 2; see Fig. S1A in the supplemental material). Cells containing ~3 or 4 foci were generally longer, suggesting failure of division in these cells.

The distance of the replication focus from the pole appeared to increase with the size of the cells. Figure 2A-I shows a collection of cells with single SSB foci arranged in order of size; the SSB focus appeared to move from near the pole to positions nearer the mid-

cell region as the cells grew in size. This visual pattern was confirmed by measurements made on a total of 154 single-nucleoid bacterial cells with one SSB focus; each was measured for cell length and the distance of the SSB focus from the nearest cell pole. The results were plotted as a function of cell size (Table 3 and Fig. 2A-II). The increasing distance of the SSB foci from the pole-proximal position toward the middle of the cell as the cells grew in size could indicate that the replication machinery was assembled near the pole but then moved toward the midcell during elongation as the cell grew. Figure S1B in the supplemental material shows the presence of cells with polar and midcell foci in the same field.

The above-mentioned phenomenon of polar focus formation and its distribution from pole proximal toward the midcell position is not restricted to *H. pylori* strain 26695. We performed IFA

Sharma et al.

TABLE 3 Distribution of average cell length and distance of SSB foci from the nearest pole

Group	Cell length range (μm)	Avg cell length (μm)	Avg distance from nearest pole (μm)	No. of cells
A	1.5–2	1.8	0.5	34
B	2.1–2.5	2.3	0.6	40
C	2.51–3	2.7	0.8	28
D	3.1–3.5	3.2	0.95	32
E	3.51–4	3.8	1.2	20
Total				154

analysis using anti-SSB antibody in the *H. pylori* strain B28 (an Indian isolate, kindly provided by A. Mukhopadhyay, National Institute of Cholera and Enteric Diseases [NICED], Kolkata, India) in order to rule out the possibility of any strain-specific bias in our observations. The occurrence and distribution of foci from pole proximal to midcell position and their frequencies were as observed for *H. pylori* strain 26695 (see Fig. S2 in the supplemental material).

The second category of cells with one SSB focus located between two lobes of almost segregated or even divided nucleoids were invariably longer than those with the SSB foci at or near a pole. Figure 2B shows undivided cells with the midcell SSB focus localized between segregated nucleoids, often attached closer to one of the nucleoids. Colocalization of DnaB and SSB foci at this position confirms ongoing replication activity at these sites (Fig. 2B).

In order to examine the position of the replication focus relative to the septal site in a dividing cell, cells were stained with the membrane marker dye FM 1-43FX, which showed the septal membrane between the two nucleoid lobes in binucleoid cells, with indications of septal invagination (Fig. 2C-I). The SSB foci in binucleoid cells were found on one side of the septum, as shown in Fig. 2C-II. We suggest that they might represent the replication forks at the terminus yet to be resolved into daughter chromosomes.

Overall, ~6% of the cells showed SSB/DnaB foci using an immunofluorescence assay. This low frequency might be due to the limitation of the IFA or caused by the unusually long generation time of slowly growing *H. pylori* cells, as previously reported (37). We also determined the generation time (t_g) of *H. pylori* cells from the linear segment of the growth curve ($\log_2$ OD$_{600}$ values plotted against time [see Fig. S3A in the supplemental material]). *H. pylori* strain 26695 showed a generation time of ~4.8 h under our experimental conditions (see Fig. S3 in the supplemental material). The C period, the time required to complete one round of replication of the *H. pylori* chromosome, could not be estimated in the absence of any reliable method for synchronization of the *H. pylori* culture. However, a rough estimate of the C period as a fraction of the generation time could be obtained from EdU labeling of a population of cells from an exponentially growing culture (see below).

EdU labeling to mark active replication sites. In order to confirm that the SSB and DnaB foci in the immunofluorescence images were indeed sites of ongoing DNA synthesis, we performed EdU (Molecular Probes) labeling of the growing replication forks in *H. pylori* cells. EdUs are thymidine analogs directly incorporated into the newly synthesized DNA at the active replication fork. EdU labeling is more efficient than bromodeoxyuridine (BrdU) labeling, since its detection is chemical and not dependent on antibody, as in the case of BrdU.

Incubation of growing *H. pylori* cells in the presence of EdU followed by chemical treatment of EdU-labeled DNA allowed visualization of active replication forks under the fluorescence microscope. Over a thousand cells were screened for the presence of EdU foci marking the active replication forks; ~9 to 10% of them showed distinct EdU foci. About 75% of these focus-containing cells were either mononucleoid, shorter cells with a single polar focus (Fig. 3, top two rows) or binucleoid, longer cells with a single focus near the midcell region (Fig. 3, bottom two rows). There is a striking similarity between the EdU focus-containing cells and SSB focus-containing cells, where ~82% of the cells with foci show a single focus either near the pole (mononucleoid cells) or near the midcell position (binucleoid cells) (Table 2). Interestingly, the single EdU focus was somewhat closer to one of the nucleoids in binucleoid cells (Fig. 3), as was also shown in SSB focus-containing binucleoid cells. The rest of the cells (~25%) with EdU foci either showed two foci in binucleoid cells or multiple foci with undivided multinucleoid cells (data not shown). Thus, EdU labeling confirms the results obtained by the SSB and DnaB immunofluorescence assays, indicating that these foci are a true representation of active replication sites.

Location of *oriC* during chromosome replication in *H. pylori* cells. The position of *oriC* was localized in fixed bacterial cells by FISH, using a fluorescence-tagged DNA sequence complementary to the target site (*oriC*), as described in Materials and Methods. After hybridization, the *oriC* region showed up as a single sharp focus and could be followed by fluorescence microscopy. Bacterial cells with clear FISH signals were photographed, and the images
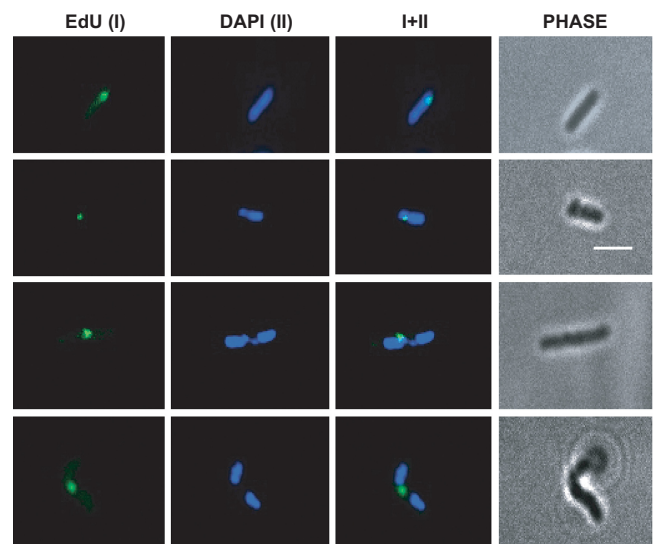

FIG 3 Visualization of active replication forks in EdU-labeled cells. *H. pylori* cells were grown in the presence of EdU, followed by fixation of the cells using formaldehyde. Chemical activation of fluorescence from EdU-labeled DNA was performed as described in Materials and Methods; EdU-labeled replication sites were then visualized by fluorescence microscopy. Column I shows the EdU foci; column II shows the DAPI-stained nucleoid(s); column III shows the merged fluorescence of I and II, while the rightmost column shows the phase-contrast images of the cells. The top two rows show polar foci in single-nucleoid cells, whereas the bottom two rows show the position of the replisome in binucleoid cells. Scale bar, 2 μm.
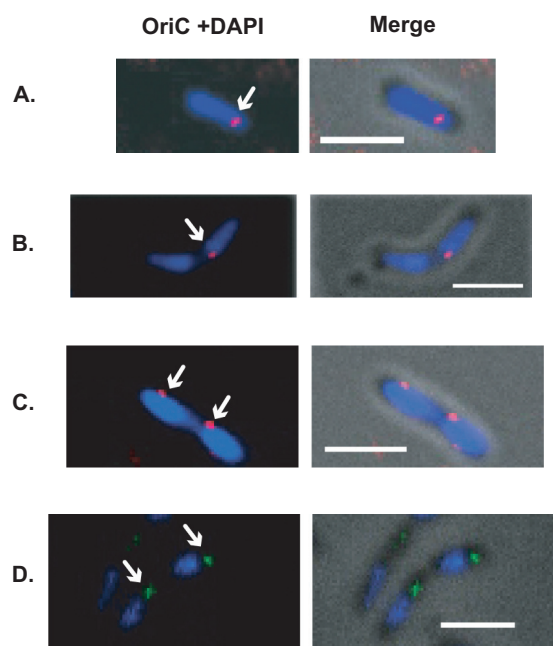
FIG 4 Position of *oriC* in *H. pylori* cells localized by FISH. (A) Single *oriC* spot in a one-nucleoid cell. (B) Single *oriC* spot in a binucleoid cell. (C) Two *oriC* spots in binucleoid cells. (D) *oriC* spots in newly divided cells. The images on the left show FISH fluorescence, while those on the right show fluorescence superimposed on phase-contrast. Scale bars, 2 μm. The arrows mark the *oriC*. FISH experiments were repeated many times with different fluorophores depending on the availability. The fluorophore used in panel D is different from that used in panels A to C.

were analyzed for the position of the Hp*oriC*. A single *oriC* focus was seen in most mononucleoid and some binucleoid cells. Two Hp*oriC* foci were seen only in binucleoid cells, with one *oriC* focus associated with each of the nucleoids. Figure 4 shows all the combinations of *oriC* and nucleoid positions seen, and Table 4 shows the frequency of each type out of 235 cells analyzed. About 35% of all cells were mononucleoid, with the *oriC* region localized at the polar edge of the nucleoid (Fig. 4A and Table 4). Similar-size cells with one nucleoid and two *oriC* foci were not seen. Longer, undivided cells (with one bilobed nucleoid or two separated nucleoids) with one *oriC* focus in the middle occurred with almost the same frequency (33%) (Fig. 4B and Table 4). Two *oriC* foci with one attached to each of the segregated nucleoid in still undivided cells were also almost equally frequent (25%) (Fig. 4C and Table 4). Longer cells at an advanced stage of division, with distinctly separated nucleoids, had one *oriC* focus located at the polar edge of each nucleoid (Fig. 4D). A few dividing cells (~6%) with bipolar *oriC* spots or more than two *oriC* spots could be seen; we have no clear explanation for this pattern at present. The presence of *oriC*

at one of the cell poles (Table 4) and the polar presence of the replication foci in the smaller cells in an exponential culture of *H. pylori* may suggest that replication is initiated at *oriC* localized near the cell pole.

Since all the cells undergoing replication could be expected to have at least two copies of the replication origin, the high frequency (~68%) of single *oriC* foci in mono- and binucleoid cells and the absence of any mononucleoid cell with two *oriC* foci is surprising. This suggests that the two copies of the *oriC* region, even if duplicated early, remain close enough together to appear as a single focus and do not separate until after the completion of elongation, when the replication forks reach the terminus and segregation is almost complete (bilobed and separated nucleoids). Subsequently, they would move with the segregated nucleoids and partition into the daughter cells (Fig. 4B to D). The prolonged association of the duplicated *oriC* regions through elongation might suggest a centromere-like sister chromatid cohesion of this segment of the *H. pylori* chromosome. However, further experiments are required to resolve these issues.

Positions of flagella during growth and division. The spiral vegetative *H. pylori* cells have asymmetric poles, only one of which has flagella that help propel the cell in the gut. The nonflagellar end helps the bacterium to adhere to the epithelial cells. To distinguish whether SSB focus formation has any preference for the flagellar or the nonflagellar end, we marked the flagellar end of *H. pylori* cells using antibodies against the basal flagellar protein HpFlgE. Polyclonal antibodies were generated by injecting purified recombinant His$_6$-HpFlgE into rabbits. The specificity of these antibodies is indicated by (i) the specific recognition of the purified protein, (ii) the specific recognition of a single band in the *H. pylori* lysate with appropriate molecular weight, and (iii) the inability of the preimmune sera to recognize the protein (Fig. 5A). These antibodies were also used in immunofluorescence assays and detected the flagellar pole in single-nucleoid cells and the bipolar flagellar ends in a majority of double-nucleoid cells (Fig. 5B). Anti-HpFlgE antibodies were further used for immunolocalization assays, along with antibodies against SSB, to analyze whether the polar SSB foci show any bias for the flagellar end. The immunofluorescence assays showed a distinct signal for SSB, as well as for FlgE (Fig. 5C). An SSB polar focus could be seen at both the flagellar and nonflagellar ends at similar frequencies (data not shown). This suggests that Hp*oriC* had equal probability to be at the flagellar or the nonflagellar end; the replisome could thus be assembled at either end without any polar bias in those cells where foci were seen. Preimmune sera did not reveal any fluorescence signals under the same experimental conditions (data not shown).

Membrane association of the *H. pylori* replisome. In order to test the probable membrane association of the replication complexes, *H. pylori* cells were fractionated into cytosolic and mem-

TABLE 4 Frequencies of occurrence of localization patterns of *oriC* spots detected by FISH

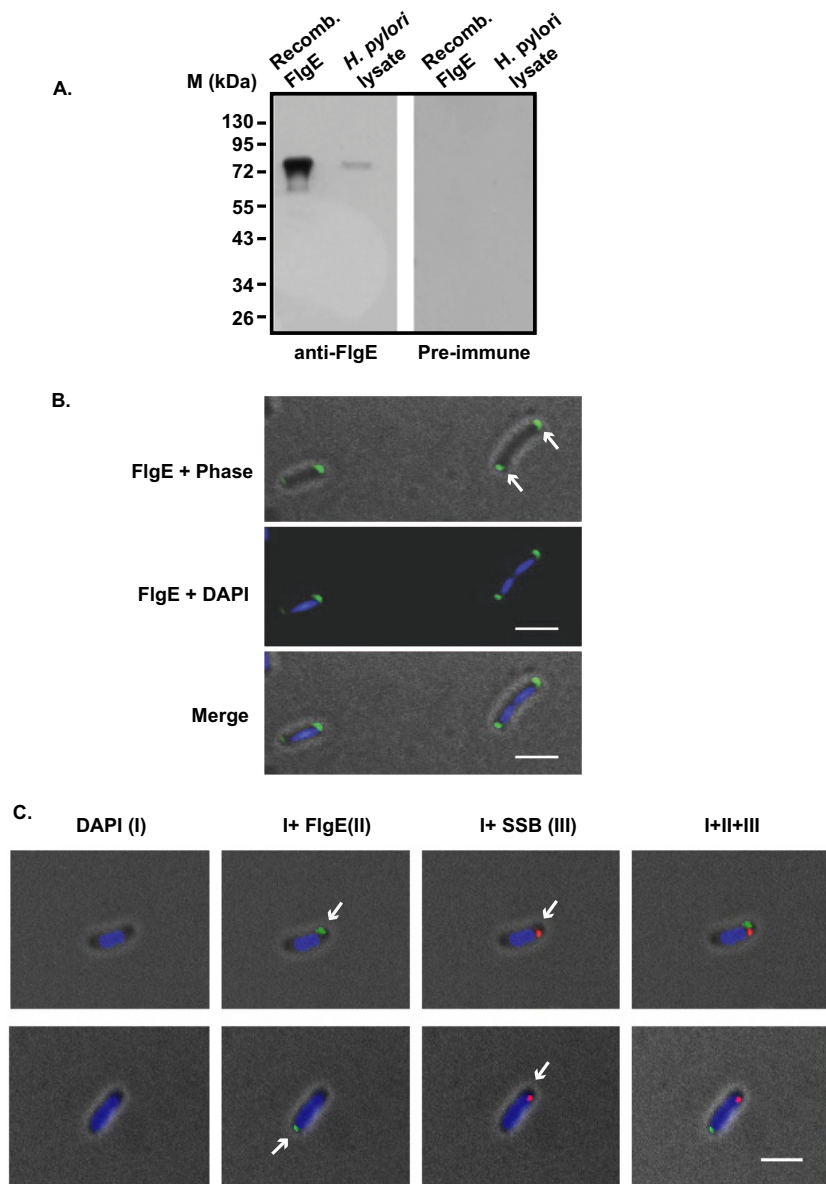| No. of nucleoids and organization	No. of *oriC*	Position with nucleoid	No. of cells	Frequency (%)	Representative image
1	1	Edge of nucleoid	89	35.6	Fig. 4A
2 (segregated in undivided cells)	1	Between segregated nucleoids	82	32.8	Fig. 4B
	2	Associated with nucleoids	64	25.6	Fig. 4C

FIG 5 Investigation of the polar bias for replisome assembly in *H. pylori*. (A) Western blot analysis using polyclonal antibodies against FlgE showed the presence of a single band corresponding to FlgE in the bacterial lysate, as well as in the purified recombinant protein lane (left). On the right is the control with preimmune sera under identical experimental conditions. (B) Immunolocalization of FlgE showing the flagellar position at one end in single-nucleoid cells and bipolar flagellar ends in double-nucleoid cells in the same field. (C) Immunolocalization of FlgE (green) and SSB (red) in *H. pylori* cells; no preference for replisome assembly at the flagellar or nonflagellar pole was seen. Scale bars, 2 μm; the arrows indicate the positions of the two proteins.

brane fractions by ultracentrifugation, and then the presence or absence of the components of replication machinery was examined in the respective fractions by Western blotting using polyclonal antibodies against HpDnaB, HpDnaG, and HpSSB (see Materials and Methods). Both DnaB and DnaG were found to be present in the membrane fraction, whereas SSB was found predominantly in the soluble fraction (Fig. 6A). As a control, we used antibodies against *H. pylori* HSP that showed the presence of HSP mainly in the cytosolic fraction. Thus, the replisome components DnaB and DnaG might be physically associated with the membrane. The occurrence of SSB mostly in the soluble fraction could be explained by its presence at the end of the growing replication fork on the lagging-strand template, which may not have direct

contact with the membrane. Alternatively, the association of SSB with the replisome may be loose enough for it to detach from the membrane fraction during the sonication process used to disrupt the cells.

Furthermore, in order to verify the membrane association of these proteins, we used immunoelectron microscopy to localize DnaB, DnaG, and SSB in *H. pylori* cells. We took more than 20 images in each case for the localization of the above-mentioned proteins. A majority (~80%) of the transmission electron microscopy images showed close proximity of the proteins to the membrane in transverse-section images of cells, with deposition of the colloidal gold particles near and over the membrane (Fig. 6B-I and -II). The longitudinal sections of *H. pylori* cells showed the presence of the
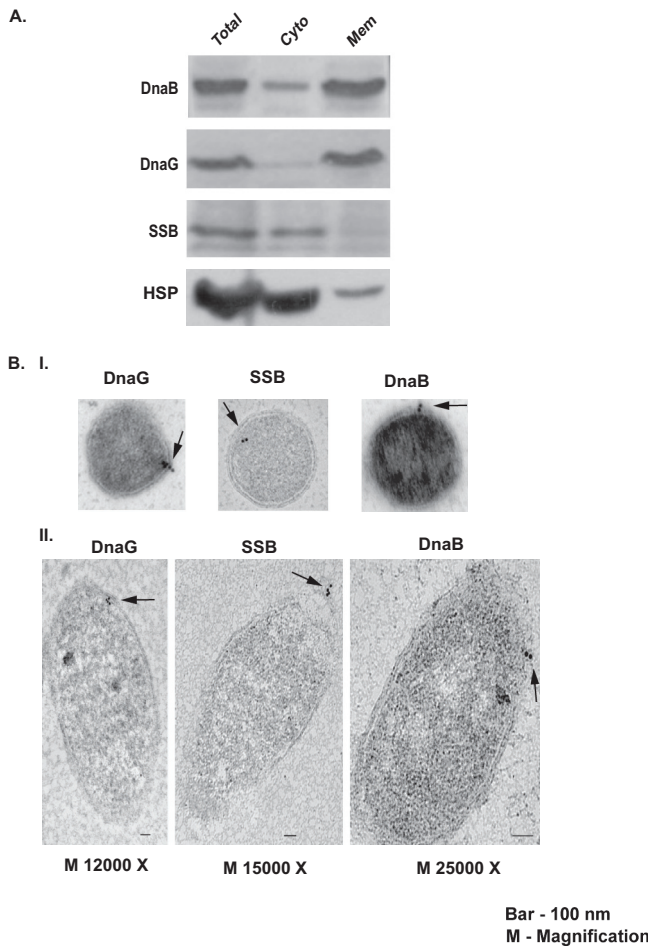
A.

DnaB

DnaG

SSB

HSP

B. I.

II.

M 12000 X   M 15000 X   M 25000 X

Bar - 100 nm
M - Magnification

FIG 6 Membrane association of replisome proteins. (A) Western blot of the subcellular fractions of *H. pylori* as described in Materials and Methods using antibodies against the proteins indicated on the left. The total lysate, cytoplasmic fraction (Cyto), and membrane fraction (Mem) were loaded in columns as indicated at the top. (B) Immunogold transmission electron microscopy. Samples were prepared as described in Materials and Methods. The deposition of the gold particles is seen in the micrographs as sharp black spots, indicating the location of the corresponding antigen (arrows). (I) Localization of DnaG and DnaB is on the membrane, while that of SSB is a little inside in transverse sections of *H. pylori* cells. (II) Membrane association and polar localization of DnaG, SSB, and DnaB in longitudinal sections of *H. pylori* cells.

replication proteins either close to the pole or at various distances from the pole toward the midcell position near the membrane. A few representative images are shown in Fig. 6B-II. The preimmune sera against these proteins did not show any gold particle deposition, suggesting the specificity of the EM results (data not shown). Thus, the replisomes appear to be attached to the membrane.

DISCUSSION

DNA replication occurs at discrete sites in living cells. The replication factors assemble stepwise from preinitiation through initiation to elongation complexes at a specific location and at a specific time in the cell cycle determined by still unclear metabolic and environmental signals (18–25) and initiate only once per generation (38). Different bacteria appear to have characteristic intracellular positions for assembly of the replisome and its movement during genome duplication. In this study, we have followed

the sequence of events from replisome assembly at initiation to termination and chromosome segregation in the slowly growing pathogen *H. pylori*, using IFA and FISH techniques to define the positions of the replication complex and the replication origin. Some of the distinguishing features observed are discussed below.

Unlike the model systems *E. coli* and *B. subtilis*, where initiation occurs from *oriC* localized at the midcell (25, 39–42), the *H. pylori* replisome is assembled at the replication origin positioned at one of the poles, as in *Caulobacter crescentus*. However, unlike *C. crescentus* (21), the location of Hp*oriC* and the assembly of the replisome are not specific for the flagellated or unflagellated pole.

The replication forks do not separate during elongation, as in *E. coli* (23), nor do they remain together fixed at the midcell position through the replication of the whole chromosome, as in *B. subtilis* (19), but move together from one pole toward the midcell until their resolution at the terminus.

Despite strong association of two major replisome components with the membrane, implying anchoring of the replication machinery, the replisome, comprising the two replication forks, moves halfway across the cell from its assembly site at the pole to the midcell region for resolution of the forks at the terminus.

Flagella are formed at the old pole of the newborn cell, but the locations of the duplicated *oriC*s are arranged in parallel positions so that they are at the flagellar and the nonflagellar poles of the daughter cells.

The predominance of single polar SSB/DnaB foci in shorter cells, together with similar localization patterns for *oriC*, indicates polar assembly of the replisome in *H. pylori* (Fig. 1 and 2). The occurrence of midcell foci in elongated and dividing *H. pylori* cells (Fig. 2B) indicates that the replisome moves from the pole toward the middle of the cell. In binucleoid cells, the SSB focus on one side of the unfinished septum could represent the last stages of replication, which include resolution of the catenated daughter chromosomes, followed by gap-filling synthesis prior to transportation of the chromosome's terminal region into one of the daughter cells by FtsK-like function, as has been reported for *E. coli* (18). Alternatively, it could represent initiation of the next round of replication of one of the daughter chromosomes before the completion of cell division. While the SSB focus moved from the pole-proximal region toward the midcell (Fig. 2A), a single *oriC* focus could be found either near the pole or near the midcell between two lobes of the nucleoid (Fig. 4). Two *oriC* foci separated only after partial separation of the daughter chromosomes and were seen in association with the two lobes of the segregated nucleoids. This pattern of *oriC* movement is different from those seen in both Gram-positive and Gram-negative model systems. In *E. coli* and *B. subtilis*, *oriC* appears in the middle of the cell at initiation (43–55). Following initiation, the duplicated *oriC*s separate and move toward opposite poles (18, 56) to take quarter positions on the longitudinal axis of the growing cell (the midcell positions of the daughter cells). The replisome remains at the midcell position throughout the round of replication in *B. subtilis* (25), while in *E. coli*, the two forks separate and move through the cell until they come together at termination (23). Initiation occurs at the *oriC* localized at the nonflagellar pole in *C. crescentus* (36, 57, 58), but after initiation, one of the duplicated *oriC*s moves rapidly to the other pole (59). The *oriC* of chromosome I of *Vibrio cholerae* is situated near the pole in the newborn cell. Following duplication, one *oriC* region travels across the cell toward the other pole, whereas the other *oriC* remains in a relatively fixed position (60).
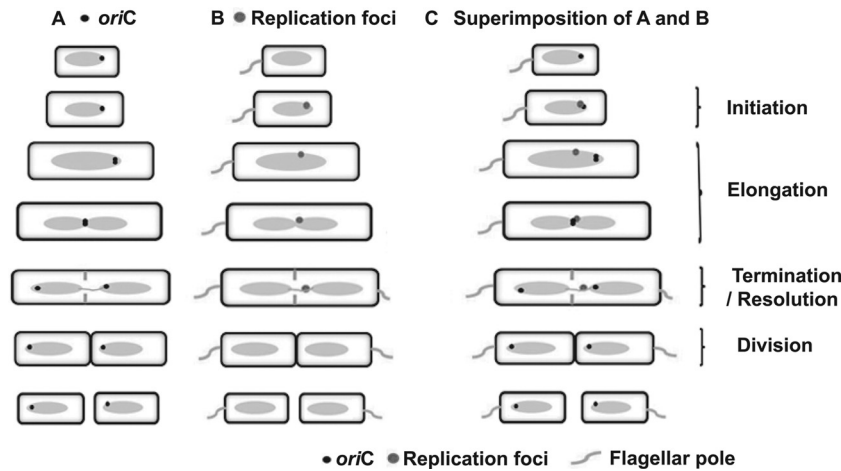
A ● *ori*C   **B ● Replication foci**   **C Superimposition of A and B**

Initiation

Elongation

Termination / Resolution

Division

● *ori*C   ● Replication foci   ⌒ Flagellar pole

FIG 7 Summary of the cell division cycle of the pathogenic bacterium *H. pylori*. Shown is a cartoon representation of intracellular localization of Hp*ori*C (based on FISH results) (A), the replication complex (based on immunofluorescence assay with antibodies against HpSSB and HpDnaB) during a single replication cycle in *H. pylori* (B), and overlap of A and B (C). The results are based on ~6% of the bacteria that showed replication foci in unsynchronized exponentially growing cultures.

H. pylori can survive and proliferate in microaerophilic environments with extremely low pH at growth rates varying from dormancy to virulence. The differences in lifestyle might necessitate the distinctive features it has acquired in replication, cell division, and their cyclic control. Furthermore, *H. pylori* is adapted to its unique niche (the gastric epithelial lining) with a fixed temperature and a long generation time (~4.8 h) compared to *E. coli*, which is a free-living bacterium with very short generation times under various temperature conditions. The polar replication focus formation and its movement toward the midcell position, as well as overall slow growth, may be an outcome of the adaptation of *H. pylori* to its unique niche, favoring its survival and growth.

Recently, Specht et al. (61) investigated the formation of the FtsZ ring and its localization in *H. pylori* cells using functional green fluorescent protein (GFP)-FtsZ protein. Unlike *E. coli* and *B. subtilis*, FtsZ in *H. pylori* localized to a single cell pole in small, newborn cells; formed spiral intermediates as the cell grew; and eventually formed imprecise rings yielding unequal daughter cells. HpFtsZ has a distinct program for polymerization and septal-ring formation, different from those of the well-studied systems of *E. coli* and *B. subtilis*.

Our observations of polar replication focus formation at one pole followed by its movement toward the cell center correlate with the polar positioning of the FtsZ ring, followed by its movement toward the midcell position. *H. pylori* shows perfect synchronization of DNA replication and cell division. It is tempting to speculate that the movements of *ori*C and the replication complex might also be guided by the cytoskeletal network that regulates the formation and localization of FtsZ rings, thus coordinating genome duplication and cell division with cellular growth in *H. pylori*.

The persistent sister chromatid cohesion of the Hp*ori*C region may suggest the presence of centromeric regions adjacent to or overlapping the replication origin. Centromeric properties have been attributed to *ori*C of *B. subtilis* and a 25-bp sequence near *ori*C in *E. coli* (45, 62). Different regions of sister chromatid cohesion have also been demonstrated during replication of the *E. coli* chromosome (63, 64). The bipartite Hp*ori*C shows cohesive asso-

ciation until the end of replication and a possible single-step separation at partition of the daughter chromosomes.

The coiled-coil structural maintenance of the chromosome (SMC) or MukB protein is involved in chromosome condensation and segregation and cell cycle progression (65). The MukB protein is essential for chromosome partition, as mutation in the *mukB* gene results in anucleate cells (66). It remains to be seen whether there is a functional homolog of SMC/MukB in *H. pylori*, as it does not encode a clear homolog of the SMC/MukB protein. The nonseparation of *ori*C till late in the cell division cycle may require a specialized protein in *H. pylori* that facilitates sister chromatid cohesion at the end of cell division.

Overall, the EdU labeling results (Fig. 3) support the immunofluorescence results using SSB/DnaB antibodies. In both cases, a majority of the cells (~75%) show either polar foci in the smaller mononucleoid cells or midcell foci in the longer binucleoid cells. The frequency of cells containing EdU foci is higher (9 to 10%) than that of the SSB focus-containing cells (~5 to 6%). This difference may be attributed to the limitations of the antibody-based immunofluorescence assay.

Direct measurement of the time required to complete a round of chromosome replication after initiation (the C period) was not possible in the absence of any reliable method for synchronization. Considering that the *H. pylori* genome is ~1.7 Mb and its duplication proceeds at the same rate as that of *E. coli* chromosome replication (~1 kb/s), the C period for the *H. pylori* chromosome would be ~28 min. EdU incorporation results show ~10% of the cells with a growing replication fork reflecting a C period equal to 10% of the generation time (~28 min). It is possible that the *H. pylori* cells have an unusually long D period (the time required for the completion of cell division following the completion of one round of chromosomal DNA replication), as ~50% of growing cells are binucleoid/multinucleoid (Table 2), where DNA replication is finished but the cell division process has yet to be completed. A low frequency of cells showing replication foci may be the result of an unusually long (~4.8-h) generation time with a short C period but an extended D period; this implies that the replication rate for the *H. pylori* chromosome is compa-

rable to that of *E. coli* notwithstanding its long generation time. This is in contrast to the long C period (estimated to be 11 h) (67) for the slowly growing human pathogen *Mycobacterium tuberculosis* (doubling time, 24 h).

The poles are not symmetric in *H. pylori*. Attachment of the bacteria to the gastric epithelial cells occurs through its nonflagellated end (68), while the flagellar end helps to invade the mucous layer via corkscrew movement. Cellular polarity may determine the subcellular organization and functions of cellular components (20, 69). Our results from the colocalization study of HpSSB and HpFlgE (Fig. 5B and C) indicate that there is no bias for the flagellar or nonflagellar pole in terms of replisome assembly in *H. pylori*.

Our finding that HpDnaB and HpDnaG are associated with the membrane suggests that the membrane may provide mechanical support for the replisome (Fig. 6A). However, we found that SSB is mostly in the cytosol. Since SSB interacts with single-stranded DNA (ssDNA) on the lagging strand, it may not attach directly to the membrane; this would explain the presence of SSB in the soluble fraction. Alternatively, SSB may be loosely bound to the replisome, and the sonication used during cell fractionation may have led to its detachment. In *B. subtilis*, DnaG primase and DnaB helicase loader have been shown to be attached to the membrane (70, 71). Association of the replisome with the cell membrane was further confirmed by the membrane localization of DnaB and DnaG and the cytoplasmic location of SSB by immunoelectron microscopy (Fig. 6B-I). Furthermore, the EM images also supported the possibility of replisome assembly at the cell poles (Fig. 6B-II). Since these proteins interact with each other, as reported previously (12, 13), the localization of the proteins in close proximity to the cell membrane is consistent with our finding that the proteins work in close association with each other.

In *E. coli*, the association of the DnaA protein with the membrane has been reported (28). The possibility of the replisome being anchored in the cell membrane has been described both in *B. subtilis* and in *E. coli* (72, 73). Our results further support the model of anchoring the replisome via replication proteins to the cell membrane. The replication initiator protein HpDnaA has already been shown to be present in the membrane in *H. pylori* (10).

Based on the above observations, we have summarized the process of the initiation of DNA replication followed by completion of DNA replication and cell division in *H. pylori* as shown in Fig. 7. It highlights the unique features of polar replisome formation and its progression during the replication and cell division cycle in the pathogenic bacterium *H. pylori*.

ACKNOWLEDGMENTS

REFERENCES

1. **Peek RM, Jr, Blaser MJ.** 2002. *Helicobacter pylori* and gastrointestinal tract adenocarcinomas. Nat. Rev. Cancer **1**:28–37. http://dx.doi.org/10.1038/nrc703.
2. **Chen Y, Wang Y, Xu W, Zhang Z.** 2005. Analysis on the mechanism of *Helicobacter pylori*-induced apoptosis in gastric cancer cell line BGC-823. Int. J. Mol. Med. **16**:741–745.
3. **Atherton JC.** 2006. The pathogenesis of *Helicobacter pylori*-induced gastro-duodenal diseases. Annu. Rev. Pathol. **1**:63–96. http://dx.doi.org/10.1146/annurev.pathol.1.110304.100125.
4. **Dhar SK, Soni RK, Das BK, Mukhopadhyay G.** 2003. Molecular mechanism of action of major *Helicobacter pylori* virulence factors. Mol. Cell. Biochem. **253**:207–215. http://dx.doi.org/10.1023/A:1026051530512.
5. **Sharma A, Dhar SK.** 2007. *Helicobacter pylori* infection: diseases and cure—a molecular approach, p 421–457. *In* Chauhan AK, Kharkwal H, Verma A (ed), Microbes for human life. IK International Publishers, New Delhi, India.
6. **Baldwin DN, Shepherd B, Kraemer P, Hall MK, Sycuro LK, Pinto-Santini DM, Salama NR.** 2007. Identification of *Helicobacter pylori* genes that contribute to stomach colonization. Infect. Immun. **75**:1005–1016. http://dx.doi.org/10.1128/IAI.01176-06.
7. **Dorer MS, Sessler TH, Salama NR.** 2011. Recombination and DNA repair in *Helicobacter pylori*. Annu. Rev. Microbiol. **65**:329–348. http://dx.doi.org/10.1146/annurev-micro-090110-102931.
8. **Sibony M, Jones NL.** 2012. Recent advances in *Helicobacter pylori* pathogenesis. Curr. Opin. Gastroenterol. **28**:30–35. http://dx.doi.org/10.1097/MOG.0b013e32834dda51.
9. **Kusters JG, Gerrits MM, Van Strip JAG, Vandebroucke-Grauls CMJE.** 1997. Coccoid forms of *Helicobacter pylori* are the morphologic manifestation of cell death. Infect. Immun. **65**:3672–3679.
10. **Zawilak A, Durrant MC, Jakimowicz P, Backert S, Zakrzewska-Czerwinska J.** 2003. DNA binding specificity of the replication initiator protein, DnaA from *Helicobacter pylori*. J. Mol. Biol. **334**:933–947. http://dx.doi.org/10.1016/j.jmb.2003.10.018.
11. **Soni RK, Mehra P, Choudhury NR, Mukhopadhyay G, Dhar SK.** 2003. Functional characterization of *Helicobacter pylori* DnaB helicase. Nucleic Acids Res. **31**:6828–6840. http://dx.doi.org/10.1093/nar/gkg895.
12. **Sharma A, Nitharwal RG, Singh B, Dar A, Dasgupta S, Dhar SK.** 2009. *Helicobacter pylori* single-stranded DNA binding protein: functional characterization and modulation of *H pylori* DnaB helicase activity. FEBS J. **2**:519–531. http://dx.doi.org/10.1111/j.1742-4658.2008.06799.x.
13. **Kashav T, Nitharwal R, Abdulrehman SA, Gabdoulkhakov A, Saenger W, Dhar SK, Gourinath S.** 2009. Three-dimensional structure of N-terminal domain of DnaB helicase and helicase-primase interactions in *Helicobacter pylori*. PLoS One **4**:e7515. http://dx.doi.org/10.1371/journal.pone.0007515.
14. **Donczew R, Weigel C, Lurz R, Zakrzewska-Czerwinska J, Zawilak-Pawlik A.** 2012. Helicobacter pylori oriC-the first bipartite origin of chromosome replication in Gram-negative bacteria. Nucleic Acids Res. **40**:9647–9660. http://dx.doi.org/10.1093/nar/gks742.
15. **Zawilak-Pawlik A, Kois A, Stingl K, Boneca IG, Skrobuk P, Piotr J, Lurz R, Zakrzewska-Czerwińska J, Labigne A.** 2007. HobA: a novel protein involved in initiation of chromosomal replication in *Helicobacter pylori*. Mol. Microbiol. **65**:979–994. http://dx.doi.org/10.1111/j.1365-2958.2007.05853.x.
16. **Soni RK, Mehra P, Choudhury NR, Mukhopadhyay G, Dhar SK.** 2005. *Helicobacter pylori* DnaB helicase can bypass *Escherichia coli* DnaC function *in vivo*. Biochem. J. **389**:541–548. http://dx.doi.org/10.1042/BJ20050062.
17. **Nitharwal RG, Paul S, Dar A, Choudhury NR, Soni RK, Prusty D, Sinha S, Kashav T, Mukhopadhyay G, Chaudhuri TK, Gourinath S, Dhar SK.** 2007. The domain structure of *Helicobacter pylori* DnaB helicase, the N-terminal domain can be dispensable for helicase activity whereas the extreme C-terminal region is essential for its function. Nucleic Acids Res. **35**:2861–2874. http://dx.doi.org/10.1093/nar/gkm167.
18. **Lau IF, Filipe SR, Søballe B, Økstad OA, Barre FX, Sherratt DJ.** 2003. Spatial and temporal organization of replicating *Escherichia coli* chromo-

somes. Mol. Microbiol. **49:**731–743. http://dx.doi.org/10.1046/j.1365
-2958.2003.03640.x.

19. **Berkmen MB, Grossman AD.** 2006. Spatial and temporal organization of the *Bacillus subtilis* replication cycle. Mol. Microbiol. **62:**57–71. http://dx.doi.org/10.1111/j.1365-2958.2006.05356.x.

20. **Dworkin, J.** 2009. Cellular polarity in prokaryotic organisms. Cold Spring Harb. Perspect. Biol. **1:**a003368. http://dx.doi.org/10.1101/cshperspect.a003368.

21. **Jensen RB, Wang SC, Shapiro L.** 2001. A moving DNA replication factory in *Caulobacter crescentus*. EMBO J. **20:**4952–4963. http://dx.doi.org/10.1093/emboj/20.17.4952.

22. **Koppes LJ, Woldringh CL, Nanninga N.** 1999. *Escherichia coli* contain a DNA replication compartment in the cell center. Biochimie **81:**803–810. http://dx.doi.org/10.1016/S0300-9084(99)00217-5.

23. **Reyes-Lamothe R, Possoz C, Danilova O, Sherratt DJ.** 2008. Independent positioning and action of *Escherichia coli* replisomes in live cells. Cell **133:**90–102. http://dx.doi.org/10.1016/j.cell.2008.01.044.

24. **Reyes-Lamothe R, Sherratt DJ, Leake MC.** 2010. Stoichiometry and architecture of active DNA replication machinery in *Escherichia coli*. Science **328:**498–501. http://dx.doi.org/10.1126/science.1185757.

25. **Lemon KP, Grossman AD.** 1998. Localization of bacterial DNA polymerase: evidence for a factory model of replication. Science **282:**1516–1519. http://dx.doi.org/10.1126/science.282.5393.1516.

26. **Harlow E, Lane D.** 1988. Antibodies: a laboratory manual. Cold Spring Harbor Laboratory Press, Cold Spring Harbor, NY.

27. **Niki H, Hiraga S.** 1997. Subcellular distribution of actively partitioning F plasmid during the cell division cycle in *E. coli*. Cell **90:**951–957. http://dx.doi.org/10.1016/S0092-8674(00)80359-1.

28. **Newman G, Crooke E.** 2000. DnaA, the initiator of *Escherichia coli* chromosomal replication, is located at the cell membrane. J. Bacteriol. **182:**2604–2610. http://dx.doi.org/10.1128/JB.182.9.2604-2610.2000.

29. **Yoshida M, Wakatsuki Y, Kobayashi Y, Itoh T, Murakami K, Mizoguchi A, Usui T, Chiba T, Kita T.** 1999. Cloning and characterization of a novel membrane-associated antigenic protein of *Helicobacter pylori*. Infect. Immun. **67:**286–293.

30. **Baik SC, Kim KM, Song SM, Kim DS, Jun JS, Lee SG, Song JY, Park JU, Kang HL, Lee WK, Cho MJ, Youn HS, Ko GH, Rhee KH.** 2004. Proteomic analysis of the sarcosine-insoluble outer membrane fraction of *Helicobacter pylori* strain 26695. J. Bacteriol. **186:**949–955. http://dx.doi.org/10.1128/JB.186.4.949-955.2004.

31. **Fischer W, Haas R.** 2004. The RecA protein of *Helicobacter pylori* requires a posttranslational modification for full activity. J. Bacteriol. **186:**777–784. http://dx.doi.org/10.1128/JB.186.3.777-784.2004.

32. **Carlsohn E, Nyström J, Karlsson H, Svennerholm AM, Nilsson CL.** 2006. Characterization of the outer membrane protein profile from disease-related *Helicobacter pylori* isolates by subcellular fractionation and nano-LC FT-ICR MS analysis. J. Proteome Res. **5:**197–204. http://dx.doi.org/10.1021/pr060181p.

33. **Yao NY, O'Donnell M.** 2010. SnapShot: the replisome. Cell **141:**1088. http://dx.doi.org/10.1016/j.cell.2010.05.042.

34. **Wang X, Reyes-Lamothe R, Sherratt DJ.** 2008. Modulation of *Escherichia coli* sister chromosome cohesion by topoisomerase IV. Genes Dev. **22:**2426–2433. http://dx.doi.org/10.1101/gad.487508.

35. **Smith DH, Davis BD.** 1967. Mode of action of novobiocin in *Escherichia coli*. J. Bacteriol. **93:**71–79.

36. **Jensen RB.** 2006. Coordination between chromosome replication, segregation and cell division in *Caulobacter crescentus*. J. Bacteriol. **6:**2244–2253. http://dx.doi.org/10.1128/JB.188.6.2244-2253.2006.

37. **Vega AE, Cortinas TI, Mattana CM, Silva HJ, Centorbi OP.** 2003. Growth of *Helicobacter pylori* in medium supplemented with cyanobacterial extract. J. Clin. Microbiol. **41:**5384–5388. http://dx.doi.org/10.1128/JCM.41.12.5384-5388.2003.

38. **Boye E, Løbner-Olesen A, Skarstad K.** 2000. Limiting DNA replication to once and only once. EMBO Rep. **1:**479–483. http://dx.doi.org/10.1093/embo-reports/kvd116.

39. **Onogi T, Niki H, Yamazoe M, Hiraga S.** 1999. The assembly and migration of SeqA-Gfp fusion in living cells of *Escherichia coli*. Mol. Microbiol. **31:**1775–1782. http://dx.doi.org/10.1046/j.1365-2958.1999.01313.x.

40. **Brendler T, Sawitzke J, Sergueev K, Austin S.** 2000. A case for sliding SeqA tracts at anchored replication forks during *Escherichia coli* chromosome replication and segregation. EMBO J. **19:**6249–6258. http://dx.doi.org/10.1093/emboj/19.22.6249.

41. **Molina F, Sanchez-Romero MA, Jimenez-Sanchez A.** 2008. Dynamic organi-

42. **Wang X, Lesterlin C, Reyes-Lamothe R, Ball G, Sherratt DJ.** 2011. Replication and segregation of an *Escherichia coli* chromosome with two replication origins. Proc. Natl. Acad. Sci. U. S. A. **108:**E243–E250. http://dx.doi.org/10.1073/pnas.1100874108.

43. **Gordon GS, Sitnikov D, Webb CD, Teleman A, Straight A, Losick R, Murray AW, Wright A.** 1997. Chromosome and low copy plasmid segregation in *E coli*: visual evidence for distinct mechanisms. Cell **90:**1113–1121. http://dx.doi.org/10.1016/S0092-8674(00)80377-3.

44. **Roos M, van Geel AB, Aarsman ME, Veuskens JT, Woldringh CL, Nanninga N.** 1999. Cellular localization of *oriC* during the cell cycle of *Escherichia coli* as analyzed by fluorescent *in situ* hybridization. Biochimie **81:**797–802. http://dx.doi.org/10.1016/S0300-9084(99)00218-7.

45. **Yamaichi Y, Niki H.** 2004. *migS*, a cis-acting site that affects bipolar positioning of *oriC* on the *Escherichia coli* chromosome. EMBO J. **23:**221–233. http://dx.doi.org/10.1038/sj.emboj.7600028.

46. **Li Y, Sergueev K, Austin S.** 2002. The segregation of the *Escherichia coli* origin and terminus of replication. Mol. Microbiol. **46:**985–996. http://dx.doi.org/10.1046/j.1365-2958.2002.03234.x.

47. **Joshi MC, Bourniquel A, Fisher J, Ho BT, Magnan D, Kleckner N, Bates D.** 2011. *Escherichia coli* sister chromosome separation includes an abrupt global transition with concomitant release of late-splitting inter sister snaps. Proc. Natl. Acad. Sci. U. S. A. **108:**2765–2770. http://dx.doi.org/10.1073/pnas.1019593108.

48. **Lewis PJ, Errington J.** 1997. Direct evidence for active segregation of *oriC* regions of the *Bacillus subtilis* chromosome and co-localization with the SpoOJ partitioning protein. Mol. Microbiol. **25:**945–954. http://dx.doi.org/10.1111/j.1365-2958.1997.mmi530.x.

49. **Webb CD, Teleman A, Gordon S, Straight A, Belmont A, Lin DC, Grossman AD, Wright A, Losick R.** 1997. Bipolar localization of the replication origin regions of chromosomes in vegetative and sporulating cells of *B. subtilis*. Cell **88:**667–674. http://dx.doi.org/10.1016/S0092-8674(00)81909-1.

50. **Webb CD, Graumann PL, Kahana JA, Teleman AA, Silver PA, Losick R.** 1998. Use of time-lapse microscopy to visualize rapid movement of the replication origin region of the chromosome during the cell cycle in *Bacillus subtilis*. Mol. Microbiol. **28:**883–892. http://dx.doi.org/10.1046/j.1365-2958.1998.00808.x.

51. **Sharpe ME, Errington J.** 1998. A fixed distance for separation of newly replicated copies of *oriC* in *Bacillus subtilis*: implications for co-ordination of chromosome segregation and cell division. Mol. Microbiol. **28:**981–990. http://dx.doi.org/10.1046/j.1365-2958.1998.00857.x.

52. **Sharpe ME, Errington J.** 1999. Upheaval in the bacterial nucleoid. An active chromosome segregation mechanism. Trends Genet. **15:**70–74.

53. **Teleman AA, Graumann PL, Lin DC, Grossman AD, Losick R.** 1998. Chromosome arrangement within a bacterium. Curr. Biol. **8:**1102–1109. http://dx.doi.org/10.1016/S0960-9822(98)70464-6.

54. **Lee PS, Lin DC, Moriya S, Grossman AD.** 2003. Effects of the chromosome partitioning protein SpoOJ (ParB) on *oriC* positioning and replication initiation in *Bacillus subtilis*. J. Bacteriol. **185:**1326–1337. http://dx.doi.org/10.1128/JB.185.4.1326-1337.2003.

55. **Lee PS, Grossman AD.** 2006. The chromosome partitioning proteins Soj (ParA) and Spo0J (ParB) contribute to accurate chromosome partitioning, separation of replicated sister origins and regulation of replication initiation in *Bacillus subtilis*. Mol. Microbiol. **60:**853–869. http://dx.doi.org/10.1111/j.1365-2958.2006.05140.x.

56. **Wang X, Possoz C, Sherratt DJ.** 2005. Dancing around the divisome: asymmetric chromosome segregation in *Escherichia coli*. Genes Dev. **19:**2367–2377. http://dx.doi.org/10.1101/gad.345305.

57. **Wang SC, Shapiro L.** 2004. The topoisomerase IV ParC subunit colocalizes with the *Caulobacter* replisome and is required for polar localization of replication origins. Proc. Natl. Acad. Sci. U. S. A. **101:**9251–9256. http://dx.doi.org/10.1073/pnas.0402567101.

58. **Viollier PH, Thanbichler M, McGrath PT, West L, Meewan M, McAdams HH, Shapiro L.** 2004. Rapid and sequential movement of individual chromosomal loci to specific subcellular locations during bacterial DNA replication. Proc. Natl. Acad. Sci. U. S. A. **101:**9257–9262. http://dx.doi.org/10.1073/pnas.0402606101.

59. **Jensen RB, Shapiro L.** 1999. Chromosome segregation during the prokaryotic cell division cycle. Curr. Opin. Cell Biol. **11:**726–731. http://dx.doi.org/10.1016/S0955-0674(99)00043-5.

60. **Fogel MA, Waldor MK.** 2005. Distinct segregation dynamics of the two

Vibrio cholerae chromosomes. Mol. Microbiol. **55**:125–136. http://dx.doi .org/10.1111/j.1365-2958.2004.04379.x.

61. **Specht M, Dempwolff F, Schätzle S, Thomann R, Waidner B.** 2013. Localization of FtsZ in *Helicobacter pylori* and consequences on cell division. J. Bacteriol. **195**:1411–1420. http://dx.doi.org/10.1128/JB.01490-12.

62. **Berkmen MB, Grossman AD.** 2007. Subcellular positioning of the origin region of the *Bacillus subtilis* chromosome is independent of sequences within *ori*C, the site of replication initiation, and the replication initiator DnaA. Mol. Microbiol. **63**:150–165. http://dx.doi.org/10.1111/j.1365 -2958.2006.05505.x.

63. **Bates D, Kleckner N.** 2005. Chromosome and replisome dynamics in *E. coli*: loss of sister cohesion triggers global chromosome movement and mediates chromosome segregation. Cell **121**:899–911. http://dx.doi.org /10.1016/j.cell.2005.04.013.

64. **Adachi S, Fukushima T, Hiraga S.** 2008. Dynamic events of sister chromosomes in the cell cycle of *Escherichia coli*. Genes Cells **13**:181–197. http: //dx.doi.org/10.1111/j.1365-2443.2007.01157.x.

65. **Thanbichler M, Shapiro L.** 2006. Chromosome organization and segregation in bacteria. J. Struct. Biol. **156**:292–303. http://dx.doi.org/10.1016 /j.jsb.2006.05.007.

66. **Niki H, Imamura R, Kitaoka M, Yamanaka K, Ogura T, Hiraga S.** 1992. *E.coli* MukB protein involved in chromosome partition forms a homodimer with a rod-and-hinge structure having DNA binding and ATP/ GTP binding activities. EMBO J. **11**:5101–5109.

67. **Nair N, Dziedzic R, Greendyke R, Muniruzzaman S, Rajagopalan M, Madiraju MV.** 2009. Synchronous replication initiation in novel *Mycobacterium tuberculosis dnaA* cold-sensitive mutants. Mol. Microbiol. **71**: 291–304. http://dx.doi.org/10.1111/j.1365-2958.2008.06523.x.

68. **Segal E, Falkow S, Thompkins LS.** 1996. *Helicobacter pylori* attachment to gastric cells induces cytoskeletal rearrangement and tyrosine phosphorylation of host cell proteins. Proc. Natl. Acad. Sci. U. S. A. **93**:1259–1264. http://dx.doi.org/10.1073/pnas.93.3.1259.

69. **Ebersbach G, Jacobs-Wagner C.** 2007. Exploration into the spatial and temporal mechanisms of bacterial polarity. Trends Microbiol. **15**:101– 108. http://dx.doi.org/10.1016/j.tim.2007.01.004.

70. **Noirot-Gros MF, Dervyn E, Wu LJ, Mervelet P, Errington J, Ehrlich SD, Noirot P.** 2002. An expanded view of bacterial DNA replication. Proc. Natl. Acad. Sci. U. S. A. **99**:8342–8347. http://dx.doi.org/10.1073/pnas .122040799.

71. **Rokop ME, Auchtung JM, Grossman AD.** 2004. Control of DNA replication initiation by recruitment of an essential initiation protein to the membrane of *Bacillus subtilis*. Mol. Microbiol. **52**:1757–1767. http://dx .doi.org/10.1111/j.1365-2958.2004.04091.x.

72. **Boeneman K, Crooke E.** 2005. Chromosomal replication and the cell membrane. Curr. Opin. Microbiol. **8**:143–148. http://dx.doi.org/10.1016 /j.mib.2005.02.006.

73. **Sueoka N.** 1998. Cell membrane and chromosome replication in *Bacillus subtilis*. Prog. Nucleic Acid Res. Mol. Biol. **59**:35–53.